Published in final edited form as:
Dev Biol. 2009 February 1; 326(1): 177–189. doi:10.1016/j.ydbio.2008.11.009.

Phosphorylation of Gli2 by protein kinase A is required for Gli2 processing and degradation and the Sonic Hedgehog-regulated mouse development

Yong Pan[1], **Chengbing Wang**[1], and **Baolin Wang**[1,2,*]

1 *Department of Genetic Mediciney, Weill Medical College of Cornell University, 1300 York Avenue, W404, New York, NY 10065*

2 *Department of Cell and Developmental Biology, Weill Medical College of Cornell University, 1300 York Avenue, W404, New York, NY 10065*

Summary

In mice, Gli2 and Gli3 are the transcription factors that mediate the initial Hedgehog (Hh) signaling. In the absence of Hh signaling, the majority of the full-length Gli3 protein undergoes proteolytic processing into a repressor, while only a small fraction of the full-length Gli2 protein is processed. Gli3 processing is dependent on phosphorylation of the first four of the six protein kinase A (PKA) sites at its C-terminus. However, whether the same phosphorylation of Gli2 by PKA is required for Gli2 processing and, if so, whether such phosphorylation regulates additional Gli2 function are unknown. To address these questions, we mutated these PKA sites in the mouse *Gli2* locus to create the $Gli2^{P1\text{-}4}$ allele. $Gli2^{P1\text{-}4}$ homozygous embryos die *in utero* and exhibit exencephaly, defects in neural tube closure, enlarged craniofacial structures, and an extra anterior digit. Analysis of spinal cord patterning shows that domains of motoneurons and V2, V1, and V0 interneurons are expanded to different degrees in both $Gli2^{P1\text{-}4}$ single and $Gli2^{P1\text{-}4}$;*Shh* double mutants. Furthermore, $Gli2^{P1\text{-}4}$ expression prevents massive cell death and promotes cell proliferation in *Shh* mutant. Analysis of $Gli2^{P1\text{-}4}$ protein in vivo reveals that the mutant protein is not processed and is twice as stable as wild type Gli2 protein. We also show that the Gli2 repressor can effectively antagonize Gli2P1-4 activity. Together, these results indicate that phosphorylation of Gli2 by PKA induces Gli2 processing and destabilization in vivo and plays an important role in the Hh-regulated mouse embryonic patterning.

Keywords

Gli2; Hedgehog; neural tube

Introduction

The Hedgehog (Hh) family of secreted signaling molecules plays fundamental roles in the patterning of many embryonic structures of animals ranging from flies to humans (Hooper and

*Corresponding Author: Baolin Wang, 1300 York Avenue, W404, New York, NY 10065, Phone: 212-746-5357, Fax: 212-746-8318, Email: baw2001@med.cornell.edu.

Scott, 2005; Huangfu and Anderson, 2006; Ingham and McMahon, 2001). Hh signals by binding to and antagonizing the twelve-pass membrane protein Patched (Ptc). This alleviates the suppression of the seven transmembrane protein Smoothened (Smo), which in turn initiates an intracellular signaling cascade. In *Drosophila*, Hh signal is mediated by the zinc-finger-containing transcription factor Cubitus Interruptus (Ci). In the absence of a Hh signal, a fraction of the full-length Ci, Ci155, is proteolytically processed at its C-terminus to generate Ci75 repressor (Aza-Blanc et al., 1997). Ci155 processing requires phosphorylation of a cluster of Ser residues in the C-terminal region by protein kinase A (PKA) (Chen et al., 1999; Chen et al., 1998; Jiang and Struhl, 1998; Price and Kalderon, 1999) and subsequently by casein kinase 1 (CK1) and glycogen synthase kinase 3 (GSK3) (Jia et al., 2002; Price and Kalderon, 2002). The hyperphosphorylated Ci is then recognized by Slimb, the fly homolog of the vertebrate βTrCP protein, the substrate recognition component of the SCF (Skp1-Cul1-F-box protein) E3 ubiquitin ligase complex. This leads to partial degradation of Ci155 by proteasome (Jia et al., 2005; Smelkinson and Kalderon, 2006). In addition to its requirement for Ci155 processing, phosphorylation of Ci155 by PKA also destabilizes the protein, thus reducing its activity (Smelkinson et al., 2007). In the presence of Hh signaling, Ci proteolysis is inhibited by an unknown mechanism, and Hh target genes are activated. Thus Ci is capable of either activating or repressing Hh targets depending on the presence or absence of Hh signals.

In vertebrates, this bipartite function of Ci has been expanded into three Gli proteins: Gli1, Gli2, and Gli3 (Ruppert et al., 1990). Gli1 is a strong activator of Hh target genes, and its transcription is regulated by Hh signaling (Bai and Joyner, 2001; Dai et al., 1999; Hynes et al., 1997; Karlstrom et al., 2003; Lee et al., 1997). Gli1 does not contain a repressor domain and is not processed (Dai et al., 1999; Kaesler et al., 2000; Sasaki et al., 1999). Therefore, Gli1 is functionally analogous to the activating form of Ci155. Nevertheless, *Gli1* is dispensable in mice (Bai et al., 2002; Park et al., 2000), though not in the zebrafish (Karlstrom et al., 2003). These findings suggest that Gli1 is not essential for initial Shh signal transduction, but it is likely to enhance the expression of Hh target genes upon their initial activation by Hh signaling in the mouse.

Unlike Gli1, the majority of the full-length Gli3 protein (Gli3-190) is proteolytically processed to the Gli3 transcriptional repressor, Gli3-83, in the absence of Hh signaling (Wang et al., 2000). Gli3 processing resembles that of Ci in that it requires the phosphorylation of the first four PKA sites in its C-terminus and of multiple adjacent CK1 and GSK3 sites. Following its phosphorylation, Gli3-190 is ubiquitinated by the SCF $^{\beta TrCP}$ ubiquitin E3 ligase and is processed by proteasome in a site-specific manner (Tempe et al., 2006; Wang et al., 2000; Wang and Li, 2006). In the presence of a Hh signal, Gli3 processing is inhibited and the full-length protein is activated (Huangfu and Anderson, 2005; Litingtung et al., 2002; Wang et al., 2000). However, Gli3-190, unlike Ci155, exhibits a weak activator function *in vivo* even when it is activated (Wang et al., 2007). This finding provides an explanation for why loss-of-function mutations in *Gli3* generally result in phenotypes that resemble hyperactive Hh signaling in both mice and humans (Hui and Joyner, 1993; Vortkamp et al., 1991).

In contrast to Gli3, Gli2 is generally thought to act as a transcriptional activator. For example, mouse *Gli2* null mutation results in loss of the ventral-most cell types in the developing neural tube, which requires the highest Hh signaling activity (Ding et al., 1998; Matise et al., 1998). Moreover, expression of Gli1 in place of *Gli2* locus can rescue *Gli2* mutant phenotypes (Bai and Joyner, 2001). However, genetic studies of somite development of *Gli2* mutants in a *Gli3* null background have uncovered a weak repressor activity of Gli2 (Buttitta et al., 2003; McDermott et al., 2005). Consistent with the potential dual functions of the mouse Gli2, we have recently shown that a small fraction of Gli2 is processed *in vivo* (Pan et al., 2006). The low efficiency of Gli2 processing is determined by the processing determinant domain, or PDD, which consists of 197-amino acid residues immediately upstream of the first PKA site (Pan

and Wang, 2007). However, it remains unclear whether the phosphorylation of Gli2 by PKA is required for Gli2 processing, as it has proved to be difficult to demonstrate Gli2 processing in cultured cells overexpressing Gli2. Instead, we showed that phosphorylation of the first four PKA sites in the Gli2 C-terminus destabilizes Gli2 protein in cultured cells (Pan et al., 2006). Thus, phosphorylation of these PKA sites may potentially induce both Gli2 processing and destabilization in vivo.

To understand how phosphorylation by PKA regulates Gli2 activity, we mutated the first four PKA sites in the mouse *Gli2* locus to create the *Gli2*$^{P1-4}$ mutant allele. *Gli2*$^{P1-4}$ homozygous embryos die *in utero* and display exencephaly, defects in neural tube closure, enlarged craniofacial structures, and an extra anterior digit. Analysis of spinal cord patterning in the single and compound mutants with *Shh*$^{-/-}$ shows that Gli2^{P1-4} constitutively activates Hh target genes. Consistent with this gain of Gli2 activity, the mutant protein is not processed and gains significantly increased stability. Therefore, phosphorylation of the first four PKA sites in the Gli2 C-terminus induces both Gli2 processing and complete degradation, and thus inhibits the Gli2 transcriptional activity.

Materials and Methods

Mouse strains and the generation of the *Gli2*$^{P1-4}$ mutant knock-in allele

A PAC clone containing mouse Gli2 genomic DNA sequences (Geneservices, Inc. UK) was used to create a Gli2P1-4 targeting construct in the pGKneoloxP2DTA.2 vector (Soriano, 1997). The Gli2 construct was engineered by replacing part of the last large exon of the mouse *Gli2* gene, which contains the coding sequence for the first four PKA sites, with the corresponding mouse *Gli2* cDNA sequences containing Ser-to-Ala mutations at the first four PKA sites (Pan et al., 2006) (Fig. 1A). A *BamHI* site was introduced, without changing any codons in the region, after the sixth PKA site to facilitate identification of the mutant allele. The Gli2P1-4 construct was then introduced into R1 ES cells by electroporation, and neomycin (*neo*)-resistant clones were selected by incubating cells in ES cell growth medium containing G418 (200μg/ml). Targeted ES cell clones were identified by restriction enzyme digestion, followed by a Southern blot analysis of ES cell DNA using a 5′- and a 3′-probes. The 5′-probe identified a 6.4kb fragment in the targeted allele and a 7.8kb fragment in the wild-type (wt) allele following *XbaI* digestion. The 3′ probe identified a 9kb fragment in the targeted allele and a 7.2-kb fragment in the wt allele following *BglII* digestion (Fig. 1B). Gli2P1-4 targeted ES cell clones were obtained, and two were injected into C57BL/6 blastocysts to generate chimeric founders, which were then bred with C57BL/6 to establish F1 heterozygotes. PCR analysis was used for routine genotyping with the following primers: fwd P1, 5′-GTT ATT AGG TCC CTC GAC CTG-3′ and rev P1, 5′-CTG TCT CTT CGT TCC TGC A-3′ for the targeted allele containing the *neo* gene, which produced a 278bp fragment; and fwd P2, 5′-CTC TTC TAC CAT CGA GTG CCT-3′ and rev P2, 5′-AGA CTC CCT GAT CTG TTT CCC-3′ for wt *Gli2* allele only, which produced a 162bp fragment. *Shh* mutant mice (Chiang et al., 1996) were obtained from Philip Beachy. All mice used in this study were in a 129v and C57BL/6 mixed background.

In ovo electroporation

Mouse Gli2, Gli2P1-4, and Gli2-1-676 (1-676aa) cDNAs were separately cloned into pMIWIII, a chicken actin-promoter-based expression vector (kindly provided by Lee Niswander). For electroporation, 0.5μg/μl pMIW-Gli2, 0.5μg/μl pMIW-Gli2P1-4, or 20ng/μl pMIW-Gli2-1-676 was mixed with 2μg/μl pEGFP (Clonetech). For coelectroporation, 0.5μg/μl pMIW-Gli2 or 0.5μg/μl pMIW-Gli2P1-4 and 20ng/μl pMIW-Gli2-1-676 were mixed with 2μg/μl pEGFP at a final concentration as indicated, and the DNA mix was electroporated into one side of the neural tube of chick embryos at Hamberger & Hamilton (HH) stage 12–14

(Hamburger and Hamilton, 1992). The electroporation was performed with five 40V pulses for 50ms at 100ms intervals with the two electrodes 0.4cm apart. Embryos were sacrificed 48h later and processed for immunostaining analysis as described for mouse embryos (see below).

Immunoblotting, *in situ* hybridization, and immunohistochemistry

Detection of Gli2 proteins in E10.5 mouse embryos was performed by enrichment for Gli proteins with a Gli-binding oligonucleotide followed by immunoblotting with a Gli2 antibody or directly using protein lysates (Pan et al., 2006). In situ hybridization of cryo-tissue sections was performed as described (Schaeren-Wiemers and Gerfin-Moser, 1993)

For BrdU labeling, pregnant mice were intraperitoneally injected with BrdU (Sigma) at 100 mg per gram body weight 0.5 hr prior to dissection. For immunohistochemistry, mouse embryos at 10.5 days post coitus (E10.5) were dissected, fixed in 4% paraformaldehyde/PBS for 20–30 minutes at 4°C, equilibrated in 30% sucrose/PBS overnight at 4°C, and embedded in OCT. The frozen embryos were transversely cryosectioned at forelimb areas (10μm). The tissue sections were incubated with primary antibodies for 1 h. After extensive wash with PBS, the sections were incubated with FITC- or Rhodamine-conjugated secondary antibodies (1:250 dilution) for 1 h. Following several washes with PBS, images were captured on a CCD camera and colors were assigned for final visualization. Antibodies used for this study include: Foxa2, Nkx2.2, Isl1, MNR2, Lhx3 (Lim-3), Evx1, Pax6, Pax7, BrdU monoclonal antibodies (Developmental Study Hybridoma Bank (DSHB), Iowa); Pax6 (Covance), GFP (Santa Cruz Biotechnology, Inc), En1 (a gift from Alexandra Joyner), and Olig2 (kindly provided by Hirohide Takebayashi)(Takebayashi et al., 2000) rabbit polyclonal antibodies. The secondary antibodies were obtained from Jackson ImmunoResearch laboratories.

For TUNEL assay, tissue sections were incubated with terminal transferase (TdT) (NEB), and biotin-16-dUTP (Biotium, Inc.) at 37°C for 1 hr. Following extensive washes with PBS, the tissue sections were incubated with 1% bovine serum albumin (BSA) for 20 min at room temperature and subsequently with Rhodamine-avidin (1:400) (Rockland) at 37°C for 30 min. After washes with PBS, the tissue sections were mounted and imaged.

Results

Generation of *Gli2^{P1-4}* allele and its mutant phenotype

Gli3 processing is dependent on the phosphorylation of the first four PKA sites in its C-terminus (Tempe et al., 2006; Wang et al., 2000; Wang and Li, 2006). As these sites are conserved in the Gli2 protein, they are likely required for regulating Gli2 processing as well. We previously also showed that phosphorylation of these sites by PKA destabilizes Gli2 protein in cultured cells (Pan et al., 2006). Thus, phosphorylation of Gli2 by PKA may inhibit Gli2 activity by inducing both its processing and complete degradation. To determine how phosphorylation by PKA regulates Gli2 activity in vivo, we used a targeted gene knock-in approach to replace Ser with Ala in the first four PKA sites in the mouse *Gli2* locus to create the *Gli2^{P1-4}* mutant allele (Fig.1A–C). Gli2 protein in E10.5 wild-type (wt) and *Gli2$^{P1-4/P1-4}$* homozygous embryos was analyzed by immunoblotting with a Gli2 antibody following enrichment of Gli proteins with Gli-binding oligonucleotide. Results showed that the full-length Gli2 (Gli2-185) was detected in both the WT and mutant embryo lysates, whereas the processed Gli2 repressor (Gli2-78) was detected only in WT embryos (Fig. 1D). This indicates that the Gli2^{P1-4} protein cannot be processed to the Gli2 repressor.

Mice heterozygous for *Gli2^{P1-4}* allele containing the *neo* gene insertion were viable and displayed no discernable phenotype. However, heterozygous mice in which the *neo* cassette had been excised displayed marked growth retardation (Fig. 2A) and died 3–5 weeks after

birth. These results suggest that the *neo* insertion might affect the level of Gli2^{P1-4} expression (see below). Because of the lethality associated with removal of the *neo* cassette, only *Gli2^{P1-4}* mutant mice with *neo* insertion were used in this study.

Gli2$^{P1-4/P1-4}$ embryos died *in utero* with a wide range of abnormalities. The most prominent phenotype was exencephalic, and the midbrain exencephaly was associated with a defect in neural tube closure. In some cases, although the neural tube appeared to be closed, an opening around the midbrain and hindbrain could still be seen (Fig. 2, compare B–C to E–F). Other features include an enlarged maxillary arch and a broader nasal process (Fig. 2, compare B to E and D to G). However, the development of eyes and ears appeared normal. *Gli2$^{P1-4/P1-4}$* embryos also exhibited an extra digit in the anterior of each of the limbs (Fig. 2, inset). These phenotypes are reminiscent of those associated with hyperactive Hh signaling, indicating that the first four PKA sites in the Gli2 C-terminus are essential for Gli2 function.

Activation of the Hh pathway in *Gli2^{P1-4}* mutant

To investigate whether mutations of the first four PKA sites in Gli2 lead to activation of Shh signaling in the neural tube, we examined the expression of *Ptc* and *Gli1*, two Shh target genes (Agren et al., 2004; Goodrich et al., 1996; Marigo et al., 1996), in *Gli2$^{P1-4/P1-4}$* mice. These two genes were expressed at high levels in the ventral area of the developing neural tube of WT embryos (Fig. 3A, C); however, their expression was markedly increased throughout the *Gli2$^{P1-4/P1-4}$* mutant neural tube (Fig. 3B, D). These results indicate that Gli2^{P1-4} expression indeed results in activation of Shh signaling pathway.

Diminished apoptosis in *Gli2^{P1-4};Shh* double mutant

Loss of *Shh* gene function causes increased cell death in the neural tube and somites (Borycki et al., 1999; Litingtung and Chiang, 2000). Since expression of Gli2^{P1-4} results in increased Shh signaling activity, we tested whether Gli2^{P1-4} could suppress the massive cell death caused by loss of Shh. TUNEL staining analysis, which labels apoptotic cells, showed that *Shh$^{-/-}$* embryos exhibited more substantial cell death in the neural tube and somites than wt embryos (Fig. 4C and graph, n = 4), consistent with previous reports (Borycki et al., 1999; Litingtung and Chiang, 2000). However, in *Gli2$^{P1-4/P1-4}$*; *Shh$^{-/-}$* double mutant embryos, residual number of apoptotic cells were detected in the neural tube, and the frequency of TUNEL-positive cells was similar to that of wild-type and *Gli2$^{P1-4/P1-4}$* embryos (Fig. 4A, B, D, and graph). These results suggest that Gli2^{P1-4} expression can prevent the cell death caused by loss of Shh. This is because Gli2^{P1-4} exhibits constitutive activity that is independent of Shh.

Restoration of cell proliferation in *Gli2^{P1-4};Shh* double mutant

We noted that the size of the neural tube in *Gli2$^{P1-4/P1-4}$* embryos was frequently slightly larger than that of the wild-type (data not shown). However, the normal size of the neural tube was restored in *Gli2$^{P1-4/P1-4}$;Shh$^{-/-}$* embryos. These observations may reflect increased cell proliferation in these mutants. To investigate this possibility, we analyzed BrdU incorporation in the neural tubes of mutant and WT E10.5 embryos from the same litters. BrdU-positive cells were detected primarily in the dorsal and intermediate spinal cord with a decreasing gradient towards the ventral most region, but not in the lateral region of the neural tube (Fig. 5A–C). In *Shh$^{-/-}$* mutants, BrdU+ cells were detected in the ventricular zone at the ventral midline as the floor plate is not specified and its position is occupied by the rapidly dividing neural progenitors (Fig. 5D–F). In contrast, BrdU incorporation in the floor plate was restored in both *Gli2$^{P1-4/P1-4}$* single and *Gli2$^{P1-4/P1-4}$;Shh$^{-/-}$* double mutants (Fig. 5G–L). These results indicate that Gli2^{P1-4} expression can restore the cell proliferation of ventral spinal cord progenitors caused by the loss of Shh function, while it has little effect on proliferation of these cells in the presence of Shh.

Neural tube patterning of *Gli2*$^{P1-4}$ mutants

The spinal cord has been used as a model to study the role of Hh pathway components in embryonic patterning. Five distinct classes of neurons are generated in the ventral region of the neural tube, with floor plate (FP) forming in the ventral midline and V3 interneurons, motoneurons (MNs), V2, V1, and V0 interneurons developing in order from the ventral most to intermediate region (Jessell, 2000). Shh is expressed in the notochord and moves to the ventral neural spinal cord where it induces all ventral cell types in a concentration-dependent manner (Briscoe et al., 2000; Echelard et al., 1993; Ericson et al., 1997). Each of the five classes of cell types and FP can be marked by the expression of distinct groups of transcription factors.

To investigate whether Gli2^{P1-4} mutation has an effect on neural tube patterning, we examined the protein expression and positioning of a set of transcriptional factors that specifically mark those distinct ventral neurons in the neural tubes of *Gli2*$^{P1-4/P1-4}$ embryos. The area of Foxa2 + or Shh-expressing FP was enlarged a little bit (Fig. 6, compare E to A, R to Q). The domains of both Nkx2.2-positive V3 and Olig2-expressing MN progenitor cells were slightly dorsally expanded so that the two cell types overlapped marginally (Fig. 6, compare F to B). Consistent with this, the expression regions of both Isl1 and NMR2, two MN markers, were dorsally extended (Fig. 6, compare G to C and H to D). Similarly, the Lhx3-positive V2 interneurons were spread dorsally and laterally in the *Gli2*$^{P1-4/P1-4}$ embryo compared to those in WT neural tube (Fig. 6I and M). Furthermore, the En1- and Evx1-expressing cells, the V1 and V0 interneurons, occupied larger domains and were less clustered but intermingled in the mutant embryo (Fig. 6, compare N to J).

In addition to the markers that are activated by Shh signaling, we also examined Pax6 and Pax7 expression, which is normally restricted by Shh signaling and progressively ventrally increased (Fig. 6K and L)(Ericson et al., 1996; Goulding et al., 1993). In the *Gli2*$^{P1-4/P1-4}$ neural tube, this expression gradient of both proteins was diminished, and the ventral boundary of their expression domains was more dorsally restricted (Fig. 6, compare O to K and P to L), indicating that expression of Gli2^{P1-4} inhibits Pax6 and Pax7 expression. Together, these results indicate that expression of Gli2^{P1-4} protein leads to ectopic expansion of the FP, MNs, V3, V2, V1, and V0 interneurons or their progenitors and restriction of dorsal markers in the spinal cord.

Generation of MNs, V2, V1, and V0 interneurons in *Gli2*$^{P1-4}$*;Shh* double mutant embryos

In *Shh*$^{-/-}$ embryos, only a small number of V0 and V1 ventral neurons are specified (Chiang et al., 1996; Litingtung and Chiang, 2000). Since Gli2^{P1-4} expression ectopically activates several ventral transcription factors, we tested if this activation requires Shh. We examined the expression of the FP and V3 markers, Foxa2 and Nkx2.2, in *Shh*$^{-/-}$ and *Gli2*$^{P1-4/P1-4}$*;Shh*$^{-/-}$ embryos, and found that their expression was absent in both mutants (Fig. 7A, B, E, and F). In contrast, the expression of Olig2, Isl1 and MNR2 for progenitor and differentiated MNs was absent only in *Shh*$^{-/-}$ embryos (Fig. 7B–D), and so was the expression of Lhx3, En1, and Evx1 for V2-V0 interneurons, respectively (Fig. 7I–J). However, the expression of all of these markers was restored in the double mutant, even though their expression domains in the *Gli2*$^{P1-4/P1-4}$*;Shh*$^{-/-}$ embryos were diffuse and lacked clear boundaries, and some were intermixed (Fig. 7F–H and M–N).

In *Shh*$^{-/-}$ embryos, Pax6 and Pax7 are expressed throughout the neural tube (Chiang et al., 1996; Litingtung and Chiang, 2000)(Fig. 7K and L). However, their expression patterns in *Gli2*$^{P1-4/P1-4}$*;Shh*$^{-/-}$ double mutants were restored to the normal domains (Fig. 7O and P). Taken together, these data indicate that Gli2^{P1-4} exhibits activating function without Shh.

Gli2^{P1-4} protein is more stable than wt Gli2

Results described above indicate that Gli2^{P1-4} protein is constitutively active. Since only a small fraction of the full-length Gli2 is processed in vivo (Pan et al., 2006), the loss of the Gli2 repressor alone may not adequately account for the *Gli2^{P1-4}* mutant phenotypes. To understand the molecular basis underlying the *Gli2$^{P1-4/P1-4}$* phenotypes, we sought to investigate the biochemical property of the mutant protein. Since phosphorylation of overexpressed Gli2 by PKA induces its degradation in cultured cells (Pan et al., 2006), our study focused on the Gli2^{P1-4} protein stability. Immunoblotting analysis showed that the level of Gli2^{P1-4} protein expression in E10.5 *Gli2$^{P1-4/P1-4}$* embryos was similar to that of Gli2 protein in wt embryos (Fig. 8A, upper panel and graph). However, Northern blot analysis revealed that the level of *Gli2^{P1-4}* RNA in the mutant embryos was only half of *Gli2* RNA in wt embryos (Fig. 8A, lower panels and graph). These data indicate that Gli2^{P1-4} protein is twice as stable as the wt Gli2 and that the increased Gli2^{P1-4} protein stability compensates the reduction of its RNA level caused by the *neo* gene insertion.

To more precisely determine the stability of the Gli2^{P1-4} protein, we compared the half-life of Gli2^{P1-4} protein with that of wt Gli2 using mouse embryonic fibroblasts (MEFs) prepared from both *Gli2$^{P1-4/P1-4}$* and wt embryos. Following treatment with the protein synthesis inhibitor cycloheximide for various time points, the MEFs were lysed; the levels of Gli2 proteins were determined by immunoblotting with a Gli2 antibody (Fig. 8B, upper panel). Quantitative analysis of the immunoblotting results showed that the half-life for Gli2^{P1-4} protein was approximately 3 hours, but only 1.5 hours for wt Gli2 (Fig. 8B, lower panel). These data are in agreement with the results observed in embryos and indicate that mutation of the first four PKA sites in the Gli2 C-terminus stabilizes the protein in vivo.

To determine whether the PKA-dependent phosphorylation of Gli2^{P1-4} protein was diminished, we next compared the phosphorylation status of wt Gli2 to that of Gli2^{P1-4} from MEFs treated with forskolin (FSK, a chemical that activates adenyl cyclase and thus PKA) as measured by their migration in the gel. As expected, wt Gli2 protein exhibited a slower migrating shift, whereas the migration of Gli2^{P1-4} protein was not affected (Fig. 8C, compare lanes 1 to 2 and 3 to 4). As phosphorylation of Gli2 by PKA primes further phosphorylation by GSK3 and CK1 (Pan et al., 2006), the slow migrating species is most likely the result of phosphorylation by all three kinases. This result indicates that phosphorylation of endogenous Gli2^{P1-4} is indeed impaired. We also noticed that the stability of wt Gli2 protein was more susceptible to cell density changes than that of the mutant protein (data not shown).

The Gli2 repressor potently antagonizes the Gli2P1-4 activity

Gli2P1-4 protein is not only more stable than wt Gli2 but also is not processed. Thus, the gain-of-function phenotypes of *Gli2^{P1-4}* mutant may result from the combination of the increased stability and loss of the repressor. To assess the effect of loss of the Gli2 repressor on neural tube patterning, we decided to determine the ability of the Gli2 repressor to suppress Gli2P1-4 activity in chick neural tube. For this purpose, each of expression constructs for Gli2 and Gli2P1-4 was electroporated alone or together with various amount of the Gli2-1-676 (a repressor truncated to 676th residue from the C-terminus) expression construct into HH stage 12–14 chick neural tubes. An expression construct for green fluorescent protein (GFP) was also cotransfected to monitor the transfected cells. After the 48-hr incubation, the expression and patterning of ventral neural markers were examined by immunostaining. Transfection of 500 ng Gli2 alone was not sufficient to ectopically activate V3 interneuron marker Nkx2.2, but slightly induced ectopic expression of several ventral markers such as MNR2, Lhx3, and Nkx6.1 for MNs, V2, and V1-V2-MNs-V3 cell types, respectively (Fig. 9 A–D, compare left to right sides of the same neural tubes). Gli2 overexpression also inhibited dorsal marker Pax7 expression (Fig. 9E). In neural tubes electroporated with Gli2P1-4, the same neuronal markers

as well as Nkx2.2 were ectopically induced, and the magnitude of induction by the mutant protein was overall greater than that by Gli2 (Fig. 9F–I, compare them to 9A–D). Similarly, the dorsal marker Pax7 was suppressed (Fig. 9J). Since the expression levels of Gli2 and Gli2P1-4 were comparable (note that this Gli2 antibody does not recognize endogenous chick Gli2)(Fig. 9U, right panel), these results indicate that Gli2P1-4 mutant protein is more active than Gli2. This is most likely due to the fact that Gli2P1-4 is refractory to processing and degradation.

We next determined the inhibitory activity of Gli2-1-676 in the neural tube patterning. Transfection of 20 ng Gli2-1-676 construct was sufficient to suppress all of the ventral markers described above (Fig. 9P–S). Interestingly, it was also able to ectopically induce Pax7 expression in ventral region of the neural tube (Fig. 9T). To determine the ability of Gli2-1-676 to suppress Gli2 and Gli2P1-4 transcriptional activity, the expression of the same markers was examined in the neural tubes cotransfected with Gli2P1-4 (500 ng) and Gli2-1-676 (20 ng). The expression domains of Nkx2.2, Nkx6.1, and Pax7 were generally normal, although the areas of MNR2 and Lhx3 expression were slightly extended (Fig. 9K–O). Similar results were also obtained for chick embryos cotransfected with Gli2 and Gli2-1-676 (data not shown). To directly determine the ratio of Gli2P1-4 to Gli2-1-676 in transfected neural tubes, the levels of their expression were examined by immunoblotting (Fig. 9U, left panel and graph). Quantitative analysis showed that the ratio of Gli2P1-4 to Gli2-1-676 was approximately 4.5, which is somewhat smaller than 6.3, the ratio of the endogenous full-length Gli2 to the Gli2 repressor in the mouse embryo (Pan et al., 2006). The difference between these two ratios may be attributed to the different stability between Gli2P1-4 and wt Gli2 proteins and/or overexpression versus physiological level. Thus, the data suggest that the Gli2 repressor is potent to compete with Gli2P1-4 protein.

Discussion

Phosphorylation by PKA is required for Gli2 processing and destabilization in vivo

Genetic evidence indicates that the mouse Gli2 acts as a primary activator of Hh target genes *in vivo*, but it may also function as a weak repressor in Hh signaling (Ding et al., 1998; Matise et al., 1998); (Bai and Joyner, 2001; Buttitta et al., 2003; McDermott et al., 2005). In agreement with this view, we have recently shown that a small fraction of Gli2 is proteolytically processed into a transcriptional repressor *in vivo* (Pan et al., 2006). We also found that phosphorylation of the first four PKA sites in the Gli2 C-terminus induces its complete degradation in cultured cells. In the present study, we demonstrate that Gli2 processing is dependent on these PKA sites and that the same phosphorylation sites also regulate the stability of full-length Gli2 *in vivo*. These findings are reminiscent of those of Ci protein, whose phosphorylation by PKA has also been shown to induce both its processing and degradation (Chen et al., 1998; Jia et al., 2005; Smelkinson and Kalderon, 2006). Therefore, the dual role of PKA-mediated phosphorylation in the regulation of Gli2 and Ci functions appears to be conserved from *Drosophila* to vertebrates.

Previous studies have shown that Gli3 processing is induced by phosphorylation of the first four PKA sites in the Gli3 C-terminus and mediated by the proteasome through $SCF^{\beta TrCP}$ E3 ubiquitin ligase (Tempe et al., 2006; Wang et al., 2000; Wang and Li, 2006). The conservation of these phosphorylation sites between Gli2 and Gli3 suggests that Gli2 processing may also be catalyzed by the proteasome. This then raises a question: what determines whether Gli2 protein phosphorylated by PKA and subsequently by GSK3 and CK1 undergoes complete degradation or partial proteolysis to generate a repressor? We have previously shown that phosphorylation of each of the first four PKA sites in the Gli2 C-terminus primes the subsequent phosphorylation of the multiple adjacent GSK3 and CK1 sites (Pan et al., 2006). It is the phosphorylation of these sites that creates at least two or, most likely, more binding sites for

the $SCF^{\beta TrCP}$ E3 ubiquitin ligase. These binding sites may have different binding affinity to βTrCP, as they consist of different amino acid residues surrounding the phosphorylated Ser/Thr residues. Thus, the extent of the Gli2 C-terminal phosphorylation may determine the number and affinity of $SCF^{\beta TrCP}$ to bind Gli2, which might dictate whether phosphorylated Gli2 protein is to be degraded completely or partially. Alternatively, it may be the processing determinant domain (PDD) itself (Pan and Wang, 2007) that determines the amount of Gli2 protein undergoing the complete degradation or partial processing.

$Gli2^{P1-4}$ function and gross morphology of its mutant

Consistent with the inhibitory effect of PKA phosphorylation on Gli2 protein function, phenotypic analysis shows that *Gli2*$^{P1-4}$ mutant embryos display a broad range of abnormalities including exencephaly and defects in neural tube closure and craniofacial development (Fig. 2). Investigation of Hh target gene expression indicates that the abnormal phenotypes result from increased Hh signaling activity (Fig. 3). The expression of $Gli2^{P1-4}$ alone also rescues cell proliferation (Fig. 5) and prevents excessive apoptosis caused by the loss of Shh (Fig. 4). Furthermore, we show that most, if not all, ventral markers in the neural tube of the *Gli2*$^{P1-4}$ mutant embryos are somewhat expanded (Figs. 6 and 7). Together, these data indicate that $Gli2^{P1-4}$ is more active than wt Gli2. This elevated activity most likely results from the loss of the Gli2 repressor, increased stability, and possibly gain of transcriptional activity, although unlikely (see below). This increased protein stability may also account for the lethality of *Gli2*$^{P1-4/+}$ heterozygous mice in which the *neo* gene cassette has been removed, as the $Gli2^{P1-4}$ RNA expression is presumably no longer affected.

The exencephalic phenotype and neural tube defects in *Gli2*$^{P1-4}$ mutant appear rather severe (Fig. 2), but the abnormality in ventral neural tube patterning is relatively mild (Fig. 6). We believe that the former phenotypes are likely caused by dysregulated $Gli2^{P1-4}$ activity in the dorsal neural tube where Gli2 RNA is highly expressed (Hui et al., 1994). Since cells in the dorsal area are exposed to little Shh signals, levels of the Gli2 repressor in these cells are presumably higher than those in the ventral region of the neural tube. However, in *Gli2*$^{P1-4}$ mutant where the Gli2 repressor is lost and the mutant protein is stabilized, net Gli2 activity is high as measured by the dorsally expanded Gli1 and Ptc expression (Fig. 3). This may affect the expression of its target genes that are responsible for dorsal neural tube patterning. Genes in Wnt pathway are potential candidates, since they play an important role in determining planar cell polarity (PCP), which is essential for brain and neural tube closure (Wallingford, 2006).

It is generally thought that Gli3 is the only transcription factor that mediates Shh signaling in limb digit patterning (Litingtung et al., 2002; te Welscher et al., 2002). The role of Shh signaling in limb patterning is to create a Gli3 activator to repressor ratio gradient (Harfe et al., 2004; Wang et al., 2000; Wang et al., 2007). Although loss of Gli2 function does not alter limb patterning, *Gli2*$^{P1-4}$ mutant mice exhibit an extra digit in the anterior of each of four limbs (Fig. 2). This phenotype is most likely caused by an increase in an overall Gli activator and Gli repressor ratio. Our results thus suggest that Gli2 may also play a role in the limb patterning, which is normally masked by Gli3 function.

Does the Gli2 repressor play a role in neural tube patterning?

In *Shh* or *Smo* mutant embryos, the FP, V3, MNs, V2 ventral neural cell types are missing, and residual V1 and V0 interneurons are generated (Chiang et al., 1996; Litingtung and Chiang, 2000; Wijgerde et al., 2002). Thus, a Shh signaling gradient is required for the specification and patterning of all of these neurons during embryogenesis. From many studies of *Gli2*, *Gli3*, *Smo*, and *Shh* mutants, alone and in combination, a clear picture has emerged of the individual roles of Gli protein activities in mediating cellular responses to graded Hh signaling in the developing spinal cord (Bai et al., 2004; Ding et al., 1998; Lei et al., 2004; Litingtung

and Chiang, 2000; Matise et al., 1998; Motoyama et al., 2003; Persson et al., 2002; Wijgerde et al., 2002). Both Gli2 and Gli3 activators play the predominant roles to transduce the initial Shh signal to induce FP and V3 interneurons. Gli1, which is induced by Gli2 and Gli3, makes a minor contribution after the initial specification of these two cell types (Bai et al., 2004). Our finding that the area of V3 and FP domains is slightly expanded in *Gli2*$^{P1-4}$ mutant further supports the prevailing view that the Gli2 activator plays a predominant role in the specification of the FP and V3 neurons. However, Gli2^{P1-4} may still depend on Shh to be fully activated, since these cell types are not specified in the *Gli2*$^{P1-4}$; *Shh* double mutant (Fig. 7). Alternatively, the loss of the FP and V3 markers in the double mutant may result from the presence of the Gli3 repressor. In this case, Gli2^{P1-4} protein could have been fully activated in the absence of Shh. More genetic analysis is necessary to distinguish between these two possibilities.

The development of MNs and V2-V0 appears normal in *Gli2* mutants (Ding et al., 1998; Matise et al., 1998). However, in *Gli3* mutants and *Gli3;Shh* or *Gli3;Smo* double mutants, these cell types are generated, but their number and organization are dramatically altered (Litingtung and Chiang, 2000; Wijgerde et al., 2002). Similar phenotypes are also observed in *Gli2;Gli3* compound mutant spinal cords (Bai et al., 2004; Lei et al., 2004; Motoyama et al., 2003). Furthermore, the specification and patterning of MNs and V2-V0 appear generally normal in animals expressing only a Gli3 repressor form (Persson et al., 2002). Therefore, both the Gli2 and Gli3 activators are required for normal MN differentiation as well as V2-V0 interneuron patterning and number, but not specification. On the other hand, the Gli3 repressor, which must be suppressed to allow normal ventral cell fate development, plays an important role in the normal V2-V0 interneuron development (Litingtung and Chiang, 2000; Persson et al., 2002). From these studies, however, the function of the Gli2 repressor in neural tube patterning was not revealed. In the present study, we show that in *Gli2*$^{P1-4}$ mutant, domains of all ventral markers examined are slightly expanded, although relatively organized (Fig. 6). In addition, MNs and V2-V0 neurons are generated in *Shh*$^{-/-}$;*Gli2*$^{P1-4/P1-4}$ double mutants (Fig. 7). Since no Gli2 repressor is generated and the level of Gli2^{P1-4} protein in *Gli2*$^{P1-4/P1-4}$ embryos is similar to that of wt *Gli2*, we would argue that loss of the Gli2 repressor may have significantly contributed to the patterning of these cell types in the *Gli2*$^{P1-4}$ mutant. It should be pointed out that the premise of this argument is that mutations in the PKA sites do not increase Gli2 transcriptional activity in addition to loss of the repressor and increased stability. Our current study does not indicate whether this is the case. A recent study showed that mutations of PKA sites in Ci stabilized the protein but did not alter its transcriptional activity (Smelkinson et al., 2007). If the role of PKA-mediated phosphorylation on the regulation of Ci processing and stability is conserved in Gli2, these results would thus suggest the potential role of the Gli2 repressor in the patterning of these cell types. The fact that the Gli2 repressor activity was not revealed in the previous studies of *Gli2;Gli3*, *Gli3;Shh*, or *Gli3;Smo* double mutants suggests that the Gli2 repressor activity itself is not sufficient to influence the differentiation and patterning of these neurons. Of course, a direct test of the role of the Gli2 repressor in Hh-dependent neural tube patterning would require an additional Gli2 mutant in which the mutant protein cannot be processed but phosphorylatable by PKA.

MNs and V2-V0 interneurons in *Gli3*$^{-/-}$ spinal cord are disorganized and their number is increased as compared to those of wild-type animals (Litingtung and Chiang, 2000; Persson et al., 2002). Since Gli3 serves as the primary Gli repressor, these observations suggest that the role of the Gli repressors is to confine MNs and V2-V0 neurons in the specific regions of the neural tube. Surprisingly, in *Shh*$^{-/-}$;*Gli2*$^{P1-4/P1-4}$ double mutants, where Gli2^{P1-4} is presumably less active than in the presence of a Hh signal, the MNs and V2-V0 interneurons are generated, but they are more diffuse and disorganized than those of *Gli2*$^{P1-4}$ single mutant (compare Fig.6 to Fig.7). Therefore, the reduction of the Gli activator function also results in the mispatterning of these neurons. Together, these results support the notion that the normal

patterning of these cell types requires a precise balance between the Gli activators and repressors in any given region of the spinal cord.

Acknowledgements

We thank Alexandra Joyner for En1 antibody, Hirohide Takebayashi for Olig2 antibody, Lee Niswander for pMIWIII vector, and Aimin Liu for the help with in ovo electroporation technique. This work was supported by a NIH grant (R01GM070820) to B.W.

References

Agren M, Kogerman P, Kleman MI, Wessling M, Toftgard R. Expression of the PTCH1 tumor suppressor gene is regulated by alternative promoters and a single functional Gli-binding site. Gene 2004;330:101–14. [PubMed: 15087129]

Aza-Blanc P, Ramirez-Weber FA, Laget MP, Schwartz C, Kornberg TB. Proteolysis that is inhibited by hedgehog targets Cubitus interruptus protein to the nucleus and converts it to a repressor. Cell 1997;89:1043–53. [PubMed: 9215627]

Bai CB, Auerbach W, Lee JS, Stephen D, Joyner AL. Gli2, but not Gli1, is required for initial Shh signaling and ectopic activation of the Shh pathway. Development 2002;129:4753–4761. [PubMed: 12361967]

Bai CB, Joyner AL. Gli1 can rescue the in vivo function of Gli2. Development 2001;128:5161–5172. [PubMed: 11748151]

Bai CB, Stephen D, Joyner AL. All mouse ventral spinal cord patterning by hedgehog is Gli dependent and involves an activator function of Gli3. Dev Cell 2004;6:103–15. [PubMed: 14723851]

Borycki AG, Brunk B, Tajbakhsh S, Buckingham M, Chiang C, Emerson CP Jr. Sonic hedgehog controls epaxial muscle determination through Myf5 activation. Development 1999;126:4053–63. [PubMed: 10457014]

Briscoe J, Pierani A, Jessell TM, Ericson J. A homeodomain protein code specifies progenitor cell identity and neuronal fate in the ventral neural tube. Cell 2000;101:435–45. [PubMed: 10830170]

Buttitta L, Mo R, Hui CC, Fan CM. Interplays of Gli2 and Gli3 and their requirement in mediating Shh-dependent sclerotome induction. Development 2003;130:6233–43. [PubMed: 14602680]

Chen CH, von Kessler DP, Park W, Wang B, Ma Y, Beachy PA. Nuclear trafficking of Cubitus interruptus in the transcriptional regulation of Hedgehog target gene expression. Cell 1999;98:305–16. [PubMed: 10458606]

Chen Y, Gallaher N, Goodman RH, Smolik SM. Protein kinase A directly regulates the activity and proteolysis of cubitus interruptus. Proc Natl Acad Sci U S A 1998;95:2349–54. [PubMed: 9482888]

Chiang C, Litingtung Y, Lee E, Young KE, Corden JL, Westphal H, Beachy PA. Cyclopia and defective axial patterning in mice lacking Sonic hedgehog gene function. Nature 1996;383:407–13. [PubMed: 8837770]

Dai P, Akimaru H, Tanaka Y, Maekawa T, Nakafuku M, Ishii S. Sonic Hedgehog-induced activation of the Gli1 promoter is mediated by GLI3. J Biol Chem 1999;274:8143–52. [PubMed: 10075717]

Ding Q, Motoyama J, Gasca S, Mo R, Sasaki H, Rossant J, Hui CC. Diminished Sonic hedgehog signaling and lack of floor plate differentiation in Gli2 mutant mice. Development 1998;125:2533–43. [PubMed: 9636069]

Echelard Y, Epstein DJ, St-Jacques B, Shen L, Mohler J, McMahon JA, McMahon AP. Sonic hedgehog, a member of a family of putative signaling molecules, is implicated in the regulation of CNS polarity. Cell 1993;75:1417–30. [PubMed: 7916661]

Ericson J, Briscoe J, Rashbass P, van Heyningen V, Jessell TM. Graded sonic hedgehog signaling and the specification of cell fate in the ventral neural tube. Cold Spring Harb Symp Quant Biol 1997;62:451–66. [PubMed: 9598380]

Ericson J, Morton S, Kawakami A, Roelink H, Jessell TM. Two critical periods of Sonic Hedgehog signaling required for the specification of motor neuron identity. Cell 1996;87:661–73. [PubMed: 8929535]

Goodrich LV, Johnson RL, Milenkovic L, McMahon JA, Scott MP. Conservation of the hedgehog/patched signaling pathway from flies to mice: induction of a mouse patched gene by Hedgehog. Genes Dev 1996;10:301–12. [PubMed: 8595881]

Goulding MD, Lumsden A, Gruss P. Signals from the notochord and floor plate regulate the region-specific expression of two Pax genes in the developing spinal cord. Development 1993;117:1001–16. [PubMed: 8100762]

Hamburger V, Hamilton HL. A series of normal stages in the development of the chick embryo 1951. Dev Dyn 1992;195:231–72. [PubMed: 1304821]

Harfe BD, Scherz PJ, Nissim S, Tian H, McMahon AP, Tabin CJ. Evidence for an expansion-based temporal Shh gradient in specifying vertebrate digit identities. Cell 2004;118:517–28. [PubMed: 15315763]

Hooper JE, Scott MP. Communicating with Hedgehogs. Nat Rev Mol Cell Biol 2005;6:306–17. [PubMed: 15803137]

Huangfu D, Anderson KV. Cilia and Hedgehog responsiveness in the mouse. Proc Natl Acad Sci U S A 2005;102:11325–30. [PubMed: 16061793]

Huangfu D, Anderson KV. Signaling from Smo to Ci/Gli: conservation and divergence of Hedgehog pathways from Drosophila to vertebrates. Development 2006;133:3–14. [PubMed: 16339192]

Hui CC, Joyner AL. A mouse model of greig cephalopolysyndactyly syndrome: the extra-toesJ mutation contains an intragenic deletion of the Gli3 gene. Nat Genet 1993;3:241–6. [PubMed: 8387379]

Hui CC, Slusarski D, Platt KA, Holmgren R, Joyner AL. Expression of three mouse homologs of the Drosophila segment polarity gene cubitus interruptus, Gli, Gli-2, and Gli-3, in ectoderm- and mesoderm-derived tissues suggests multiple roles during postimplantation development. Dev Biol 1994;162:402–13. [PubMed: 8150204]

Hynes M, Stone DM, Dowd M, Pitts-Meek S, Goddard A, Gurney A, Rosenthal A. Control of cell pattern in the neural tube by the zinc finger transcription factor and oncogene Gli-1. Neuron 1997;19:15–26. [PubMed: 9247260]

Ingham PW, McMahon AP. Hedgehog signaling in animal development: paradigms and principles. Genes Dev 2001;15:3059–87. [PubMed: 11731473]

Jessell TM. Neuronal specification in the spinal cord: inductive signals and transcriptional codes. Nat Rev Genet 2000;1:20–9. [PubMed: 11262869]

Jia J, Amanai K, Wang G, Tang J, Wang B, Jiang J. Shaggy/GSK3 antagonizes Hedgehog signalling by regulating Cubitus interruptus. Nature 2002;416:548–52. [PubMed: 11912487]

Jia J, Zhang L, Zhang Q, Tong C, Wang B, Hou F, Amanai K, Jiang J. Phosphorylation by double-time/CKIepsilon and CKIalpha targets cubitus interruptus for Slimb/beta-TRCP-mediated proteolytic processing. Dev Cell 2005;9:819–30. [PubMed: 16326393]

Jiang J, Struhl G. Regulation of the Hedgehog and Wingless signalling pathways by the F-box/WD40-repeat protein Slimb. Nature 1998;391:493–6. [PubMed: 9461217]

Kaesler S, Luscher B, Ruther U. Transcriptional activity of GLI1 is negatively regulated by protein kinase A. Biol Chem 2000;381:545–51. [PubMed: 10987360]

Karlstrom RO, Tyurina OV, Kawakami A, Nishioka N, Talbot WS, Sasaki H, Schier AF. Genetic analysis of zebrafish gli1 and gli2 reveals divergent requirements for gli genes in vertebrate development. Development 2003;130:1549–64. [PubMed: 12620981]

Lee J, Platt KA, Censullo P, Ruiz i Altaba A. Gli1 is a target of Sonic hedgehog that induces ventral neural tube development. Development 1997;124:2537–52. [PubMed: 9216996]

Lei Q, Zelman AK, Kuang E, Li S, Matise MP. Transduction of graded Hedgehog signaling by a combination of Gli2 and Gli3 activator functions in the developing spinal cord. Development 2004;131:3593–604. [PubMed: 15215207]

Litingtung Y, Chiang C. Specification of ventral neuron types is mediated by an antagonistic interaction between Shh and Gli3. Nat Neurosci 2000;3:979–85. [PubMed: 11017169]

Litingtung Y, Dahn RD, Li Y, Fallon JF, Chiang C. Shh and Gli3 are dispensable for limb skeleton formation but regulate digit number and identity. Nature 2002;418:979–83. [PubMed: 12198547]

Marigo V, Johnson RL, Vortkamp A, Tabin CJ. Sonic hedgehog differentially regulates expression of GLI and GLI3 during limb development. Dev Biol 1996;180:273–83. [PubMed: 8948590]

Matise MP, Epstein DJ, Park HL, Platt KA, Joyner AL. Gli2 is required for induction of floor plate and adjacent cells, but not most ventral neurons in the mouse central nervous system. Development 1998;125:2759–70. [PubMed: 9655799]

McDermott A, Gustafsson M, Elsam T, Hui CC, Emerson CP Jr, Borycki AG. Gli2 and Gli3 have redundant and context-dependent function in skeletal muscle formation. Development 2005;132:345–57. [PubMed: 15604102]

Motoyama J, Milenkovic L, Iwama M, Shikata Y, Scott MP, Hui CC. Differential requirement for Gli2 and Gli3 in ventral neural cell fate specification. Dev Biol 2003;259:150–61. [PubMed: 12812795]

Pan Y, Bai CB, Joyner AL, Wang B. Sonic hedgehog signaling regulates Gli2 transcriptional activity by suppressing its processing and degradation. Mol Cell Biol 2006;26:3365–77. [PubMed: 16611981]

Pan Y, Wang B. A novel protein-processing domain in Gli2 and Gli3 differentially blocks complete protein degradation by the proteasome. J Biol Chem 2007;282:10846–52. [PubMed: 17283082]

Park HL, Bai C, Platt KA, Matise MP, Beeghly A, Hui CC, Nakashima M, Joyner AL. Mouse Gli1 mutants are viable but have defects in SHH signaling in combination with a Gli2 mutation. Development 2000;127:1593–605. [PubMed: 10725236]

Persson M, Stamataki D, te Welscher P, Andersson E, Bose J, Ruther U, Ericson J, Briscoe J. Dorsal-ventral patterning of the spinal cord requires Gli3 transcriptional repressor activity. Genes Dev 2002;16:2865–78. [PubMed: 12435629]

Price MA, Kalderon D. Proteolysis of cubitus interruptus in Drosophila requires phosphorylation by protein kinase A. Development 1999;126:4331–9. [PubMed: 10477300]

Price MA, Kalderon D. Proteolysis of the Hedgehog signaling effector Cubitus interruptus requires phosphorylation by Glycogen Synthase Kinase 3 and Casein Kinase 1. Cell 2002;108:823–35. [PubMed: 11955435]

Ruppert JM, Vogelstein B, Arheden K, Kinzler KW. GLI3 encodes a 190-kilodalton protein with multiple regions of GLI similarity. Mol Cell Biol 1990;10:5408–15. [PubMed: 2118997]

Sasaki H, Nishizaki Y, Hui C, Nakafuku M, Kondoh H. Regulation of Gli2 and Gli3 activities by an amino-terminal repression domain: implication of Gli2 and Gli3 as primary mediators of Shh signaling. Development 1999;126:3915–24. [PubMed: 10433919]

Schaeren-Wiemers N, Gerfin-Moser A. A single protocol to detect transcripts of various types and expression levels in neural tissue and cultured cells: in situ hybridization using digoxigenin-labelled cRNA probes. Histochemistry 1993;100:431–40. [PubMed: 7512949]

Smelkinson MG, Kalderon D. Processing of the Drosophila Hedgehog Signaling Effector Ci-155 to the Repressor Ci-75 Is Mediated by Direct Binding to the SCF Component Slimb. Curr Biol 2006;16:110–6. [PubMed: 16386907]

Smelkinson MG, Zhou Q, Kalderon D. Regulation of Ci-SCFSlimb binding, Ci proteolysis, and hedgehog pathway activity by Ci phosphorylation. Dev Cell 2007;13:481–95. [PubMed: 17925225]

Soriano P. The PDGF alpha receptor is required for neural crest cell development and for normal patterning of the somites. Development 1997;124:2691–700. [PubMed: 9226440]

Takebayashi H, Yoshida S, Sugimori M, Kosako H, Kominami R, Nakafuku M, Nabeshima Y. Dynamic expression of basic helix-loop-helix Olig family members: implication of Olig2 in neuron and oligodendrocyte differentiation and identification of a new member, Olig3. Mech Dev 2000;99:143–8. [PubMed: 11091082]

te Welscher P, Zuniga A, Kuijper S, Drenth T, Goedemans HJ, Meijlink F, Zeller R. Progression of vertebrate limb development through SHH-mediated counteraction of GLI3. Science 2002;298:827–30. [PubMed: 12215652]

Tempe D, Casas M, Karaz S, Blanchet-Tournier MF, Concordet JP. Multisite Protein Kinase A and Glycogen Synthase Kinase 3{beta} Phosphorylation Leads to Gli3 Ubiquitination by SCF{beta} TrCP. Mol Cell Biol 2006;26:4316–26. [PubMed: 16705181]

Vortkamp A, Gessler M, Grzeschik KH. GLI3 zinc-finger gene interrupted by translocations in Greig syndrome families. Nature 1991;352:539–40. [PubMed: 1650914]

Wallingford JB. Planar cell polarity, ciliogenesis and neural tube defects. Hum Mol Genet 2006;(15 Spec No 2):R227–34. [PubMed: 16987888]

Wang B, Fallon JF, Beachy PA. Hedgehog-regulated processing of Gli3 produces an anterior/posterior repressor gradient in the developing vertebrate limb. Cell 2000;100:423–34. [PubMed: 10693759]

Wang B, Li Y. Evidence for the direct involvement of {beta}TrCP in Gli3 protein processing. Proc Natl Acad Sci U S A 2006;103:33–8. [PubMed: 16371461]

Wang C, Ruther U, Wang B. The Shh-independent activator function of the full-length Gli3 protein and its role in vertebrate limb digit patterning. Dev Biol 2007;305:460–9. [PubMed: 17400206]

Wijgerde M, McMahon JA, Rule M, McMahon AP. A direct requirement for Hedgehog signaling for normal specification of all ventral progenitor domains in the presumptive mammalian spinal cord. Genes Dev 2002;16:2849–64. [PubMed: 12435628]

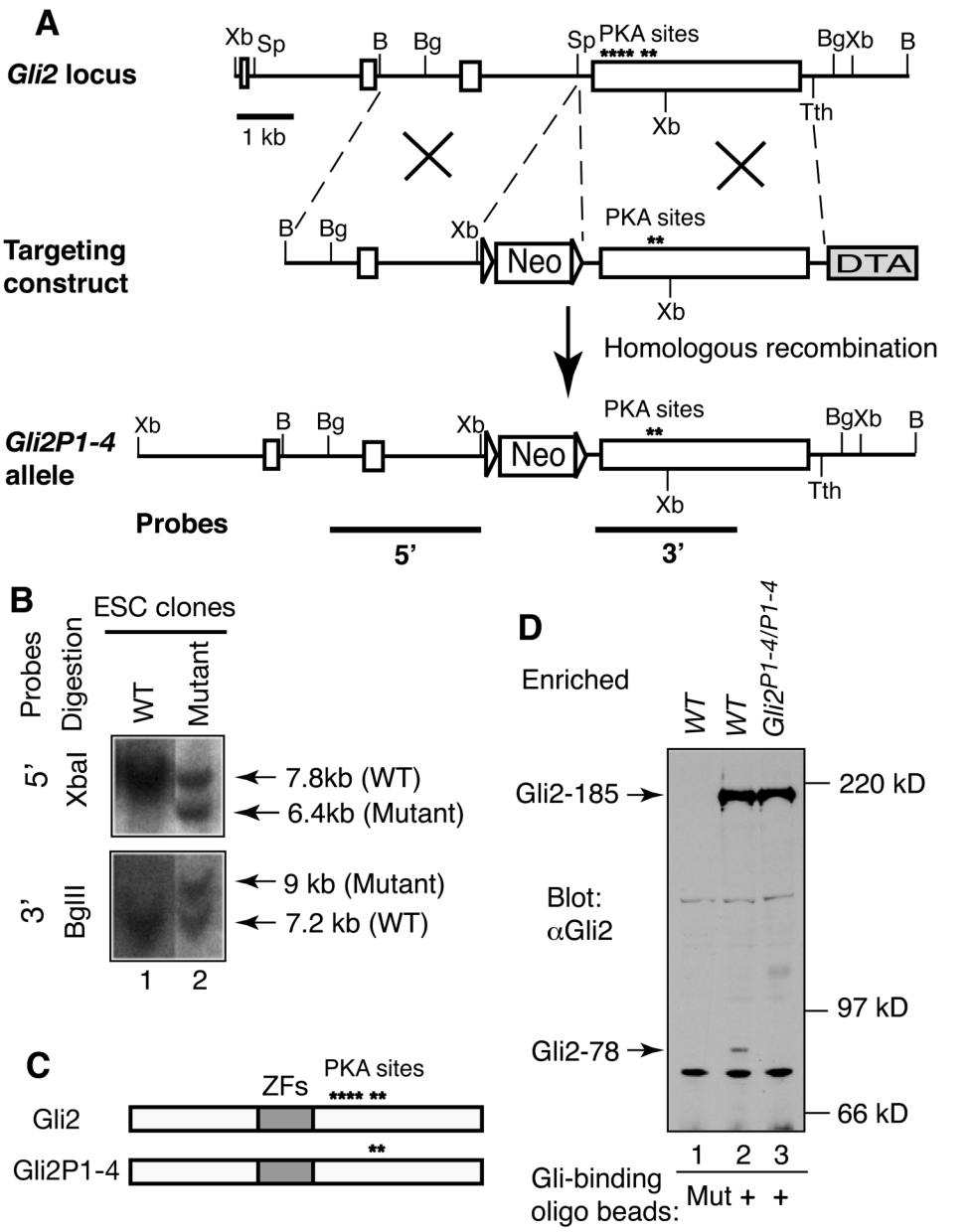

Figure 1. Generation of *Gli2*$^{P1-4}$ allele that expresses an unprocessable Gli2 protein

(**A**) The gene targeting strategy used to create *Gli2*$^{P1-4}$ allele and ES cell screening. Open boxes stand for exons, and asterisks for PKA sites. The *Gli2*$^{P1-4}$ targeting construct was created by replacing a part of the last exon of the *Gli2* gene with its corresponding cDNA sequence containing Ser-to-Ala mutations at the first four PKA sites. The *neomycin* (*neo*), which is flanked by loxP sites (triangles), and *diphtheria toxin A* (*DTA*) genes were used as positive and negative selection markers, respectively. Thick lines represent probes used for Southern blot analysis. The relevant restriction sites are: B, *BamHI*; Bg, *BglII*; Sp, *SpeI;* and Xb, *XbaI*; and Tth, *Tth111*. (**B**) Southern blot analysis of representative ES cell (ESC) clones using the 5′- and 3′-probes shown in **A** following *XbaI* and *BglII* digestion, respectively. (**C**) Diagrams showing the expected full-length Gli2 and Gli2^{P1-4} proteins. (**D**) Gli2^{P1-4} protein is not processed. Gli proteins in the lysates of E10.5 wt and *Gli2*$^{P1-4/P1-4}$ mouse embryos were first

enriched with biotinylated normal or mutated (mut) Gli-binding oligonucleotides, and Gli2 protein was then detected with a Gli2 antibody. The full-length Gli2 protein, Gli2-185, and the processed Gli2 repressor, Gli2-78, are indicated by arrows.

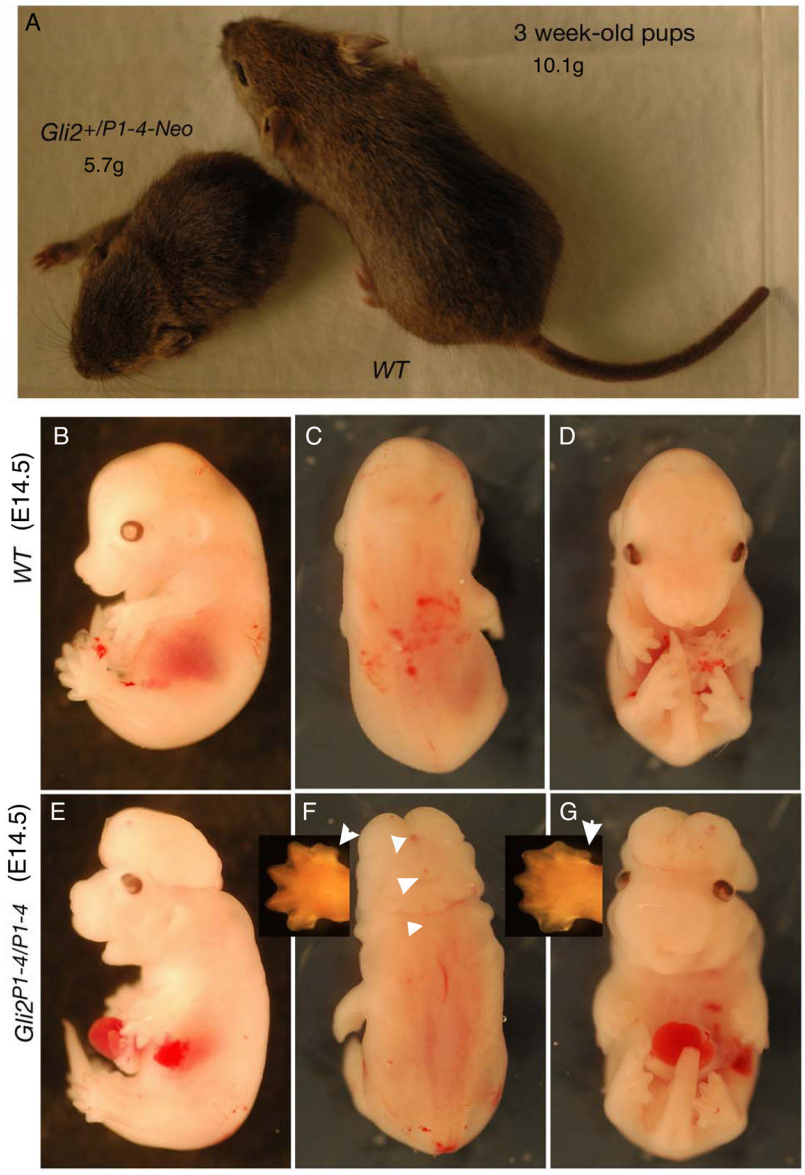

Figure 2. Phenotype of *Gli2*$^{P1-4}$ mouse mutants

(**A**) Three week old WT and *Gli2*$^{P1-4/+}$ heterozygous mice after the *neo* excision. (**B–G**) E14.5 WT and *Gli2*$^{P1-4/P1-4}$ (containing the *neo* cassette) mouse embryos from lateral (**B**, **E**), dorsal (**C**, **F**), and ventral (**D**, **G**) views. The mutant embryo displays severe exencephaly, partial opening of the neural tube (indicated by arrow heads), and enlarged maxillary, external nasal processes, and an extra anterior digit (pointed by arrows in insets).

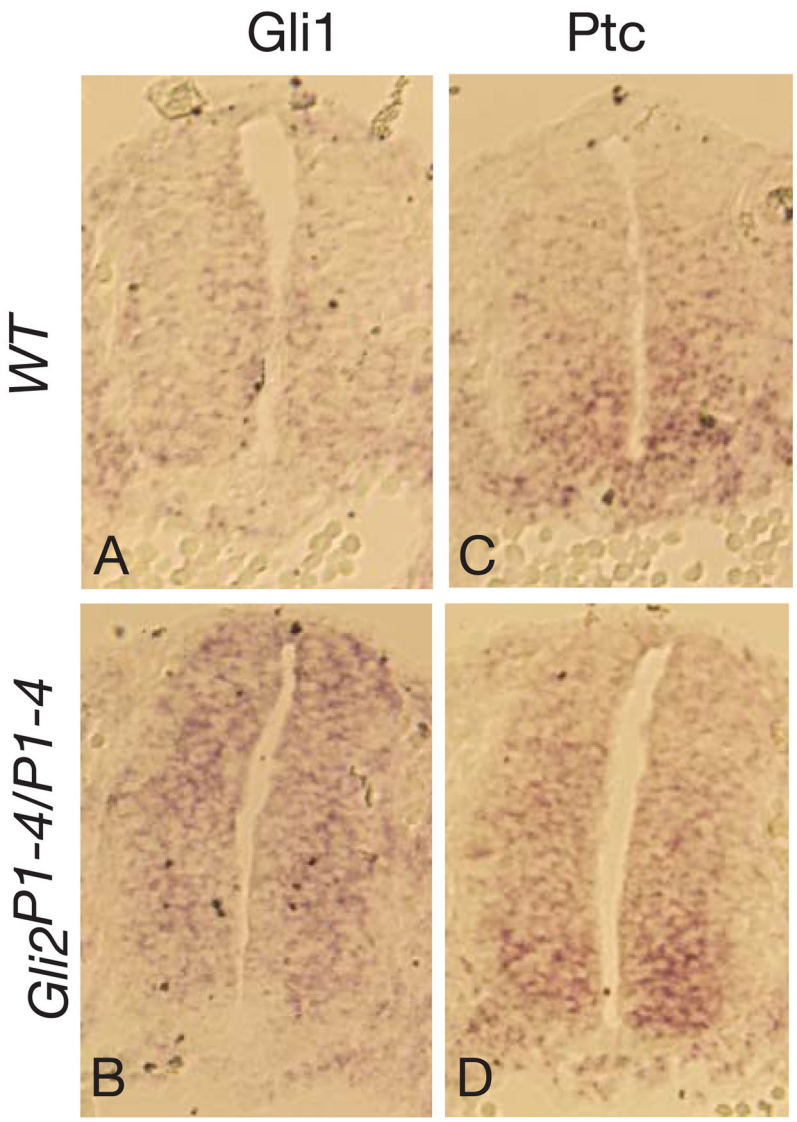

Figure 3. The Hh pathway is activated in *Gli2*$^{P1-4}$ mutant

In situ hybridization of the tissue sections (from E9.5 embryos) showing that the expression of both *Gli1* and *Ptc* RNA in wt and *Gli2*$^{P1-4}$ mutant neural tubes.

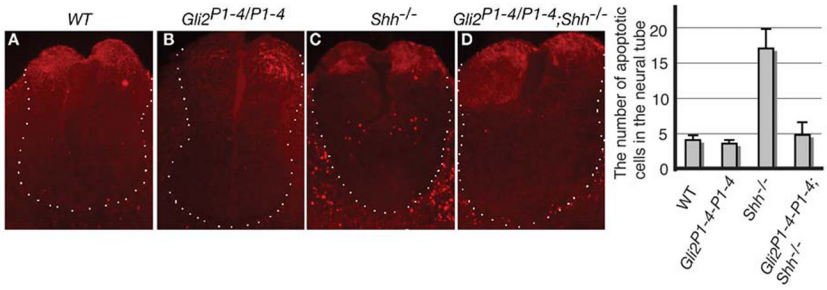

Figure 4. *Gli2*$^{P1-4}$ rescues the cell death caused by *Shh* mutation in the spinal cord

TUNEL assay was used to detect apoptotic cells in the WT (**A**), *Gli2*$^{P1-4/P1-4}$ (**B**), *Shh*$^{-/-}$ (**C**), and *Shh*$^{-/-}$;*Gli2*$^{P1-4/P1-4}$ (**D**) neural tubes of E10.5 embryos. The number of apoptotic cells within the neural tube area is shown by graph in the right (n = 4).

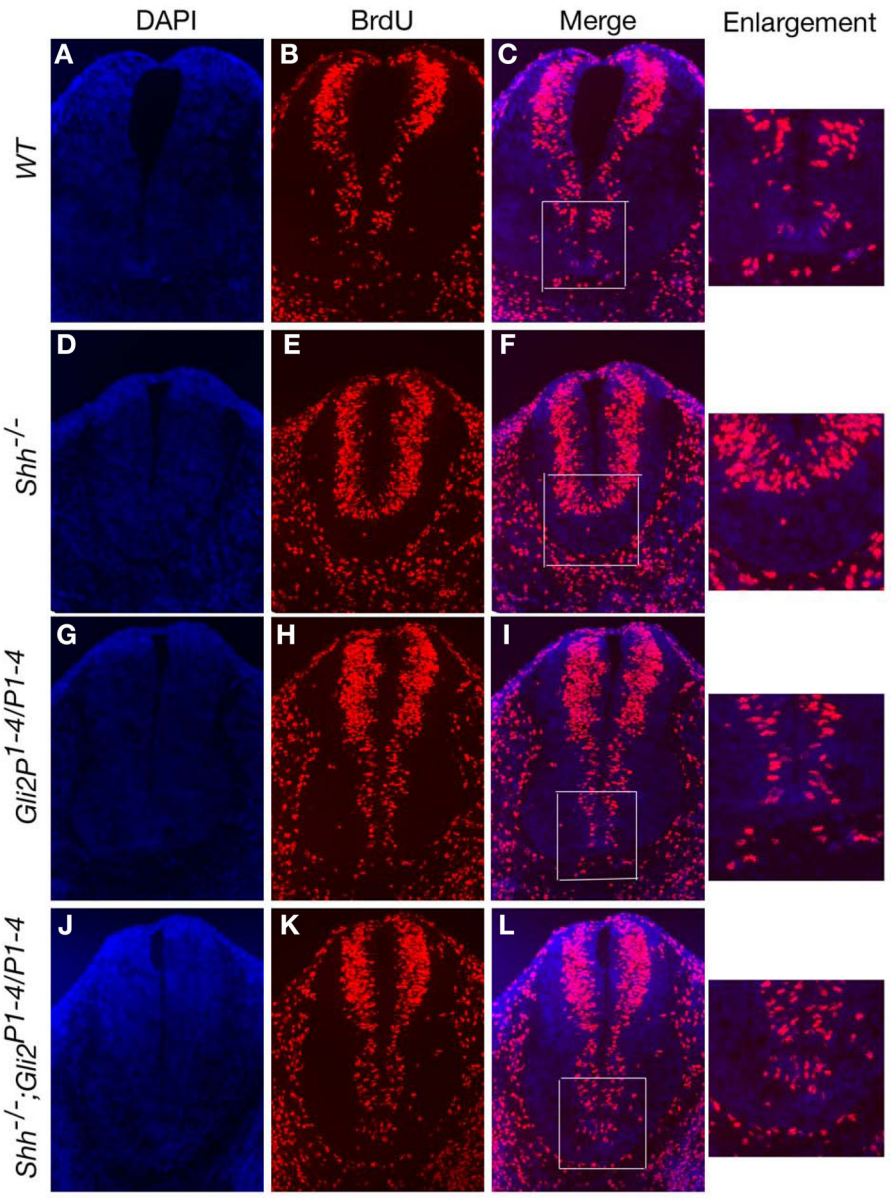

Figure 5. Cell proliferation is normal in *Gli2*$^{P1\text{-}4/P1\text{-}4}$;*Shh*$^{-/-}$ double mutant embryos

In the neural tube sections of E10.5 embryos, proliferating progenitor cells are labeled with BrdU, which is detected by immunostaining with a BrdU antibody. Nuclei are marked with DAPI. BrdU incorporation is absent in the ventral-most region of *Shh*$^{-/-}$ neural tube (**D**–**F**) as compared that in wt (**A**–**C**), but present in the *Gli2*$^{P1\text{-}4/P1\text{-}4}$ (**G**–**I**) and *Gli2*$^{P1\text{-}4/P1\text{-}4}$;*Shh*$^{-/-}$ neural tube (**J**–**L**). Enlargement of framed areas is shown to the right. BrdU+ cell numbers (about 30) in framed areas of C, I, and L are very similar.

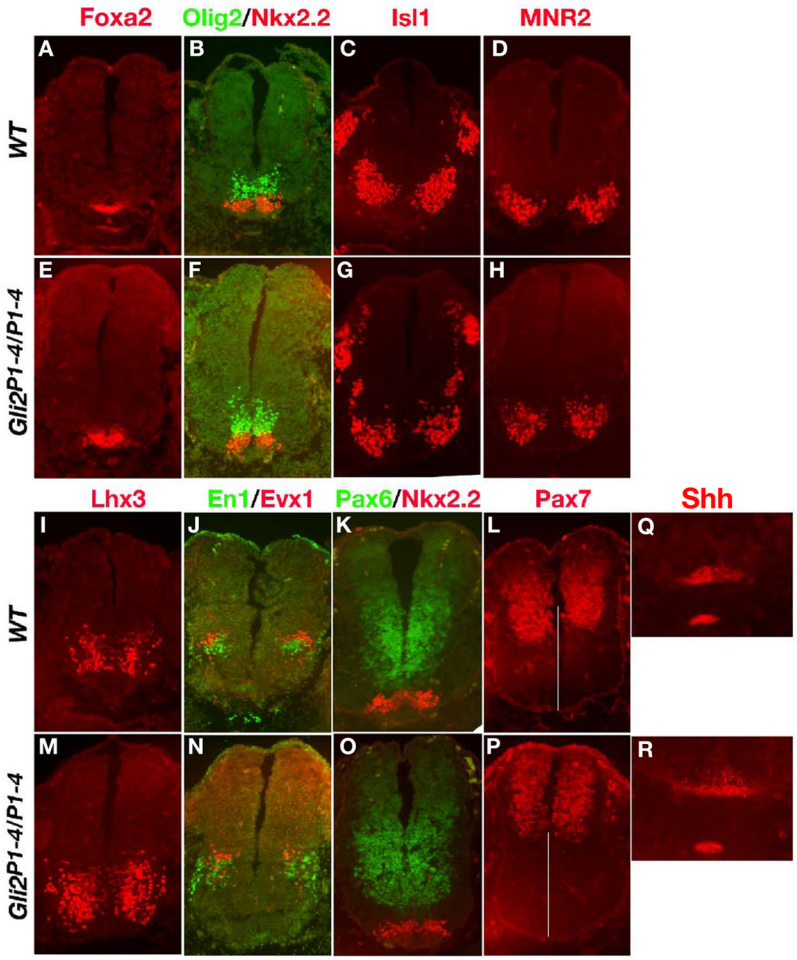

Figure 6. Abnormal neural tube patterning in the *Gli2*$^{P1-4}$ mutant

Cross-sections of E10.5 mouse embryos at the forelimb position were stained with antibodies to the proteins shown above the panels. The genotypes are indicated to the left. Note that the expression domains for Foxa2, Shh, and Nkx2.2 (the FP and V3 interneurons, respectively), Olig2 (MN progenitors), Isl1 and MNR2 (MNs), and Lhx3, En1, and Evx1 (V2, V1, and V0 interneurons, respectively) are expanded in *Gli2*$^{P1-4/P1-4}$ spinal cord, though to the different extent. Pax6 and Pax7 expression is more dorsally restricted in the mutant as measured by the white lines with the same length.

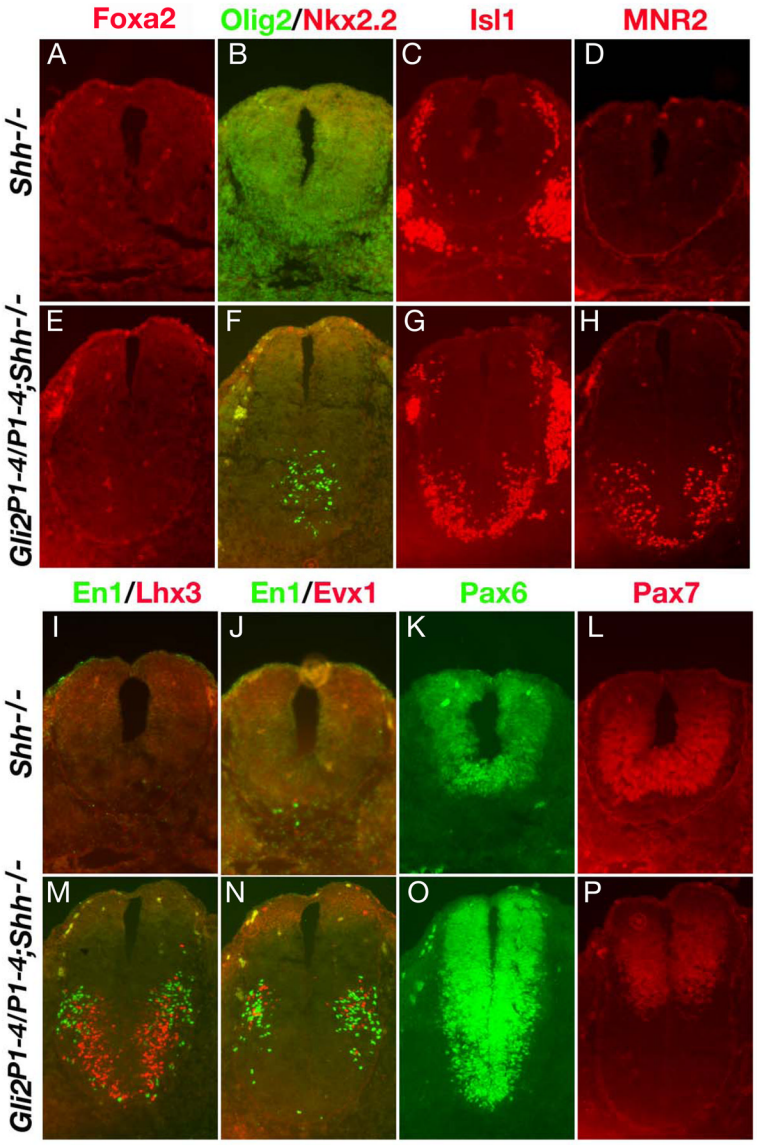

Figure 7. The specification of MNs and V0-V2 interneurons is restored in the *Gli2*$^{P1-4}$*;Shh* double mutant

Cross-sections of E10.5 mouse embryos at the forelimb position were stained with antibodies to the proteins shown above the panels. The genotypes are indicated to the left. Note that the FP and V3 interneurons (Foxa2 and Nkx2.2 expressing cells)(**A**, **B**, **E**, and **F**) are not specified in *Gli2*$^{P1-4/P1-4}$*;Shh*$^{-/-}$ embryos. However, MNs (Olig2, Isl, and MNR2 positive cells) and V2-V0 interneurons (Lhx3, En1, and Evx1 positive cells, respectively) are generated, though mispatterned (compare **F–H** to **B–D** and **I–J** to **M–N**). Similarly, the normal pattern of Pax6 and Pax7 expression is also restored (compare **O–P** to **K–L** and Fig. 6).

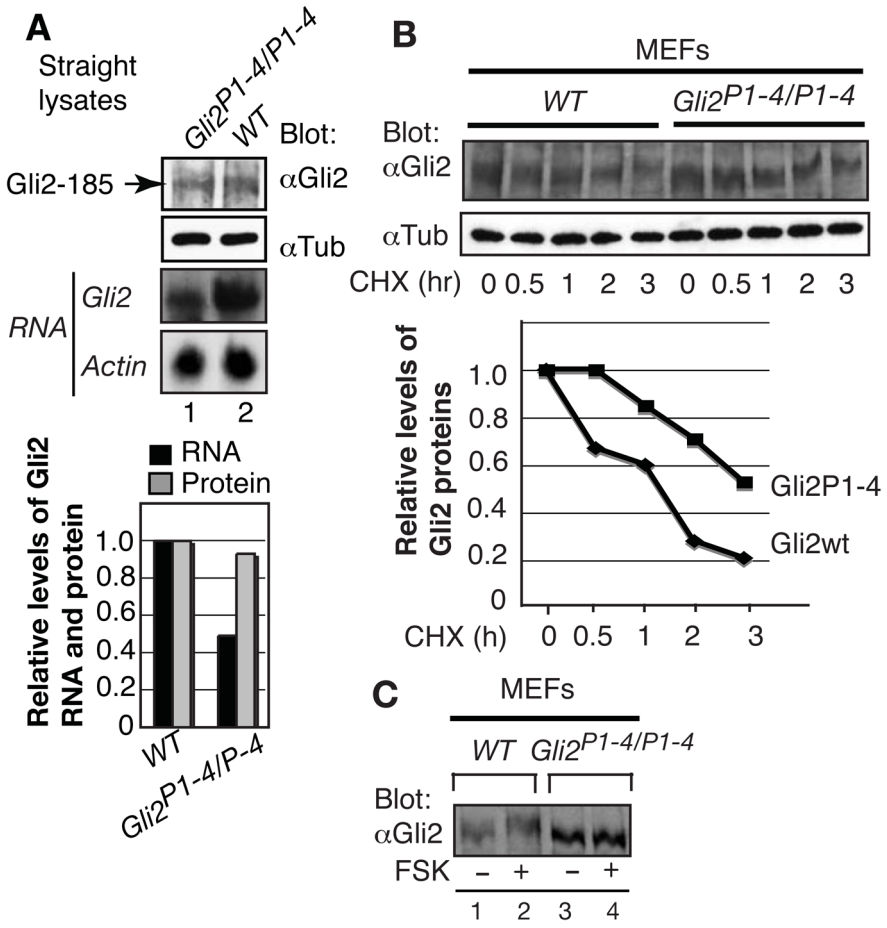

Figure 8. Gli2P-4 protein is more stable than wt Gli2

(**A**) Western and Northern blot analyses showing that the level of full-length Gli2 protein and RNA in wt and *Gli2*$^{P1-4}$ mutant embryos (E10.5). (**B**) Immunoblots showing the half-life of Gli2^{P1-4} and wt Gli2 protein in the MEFs. Cycloheximide (CHX) was used to inhibit protein synthesis. (**C**) Immunoblot showing that wt Gli2 migrated more slowly than Gli2^{P1-4} protein, when cells were treated with forskolin (FSK) overnight. Graphs show quantification of the results, and tubulin and actin are loading controls.

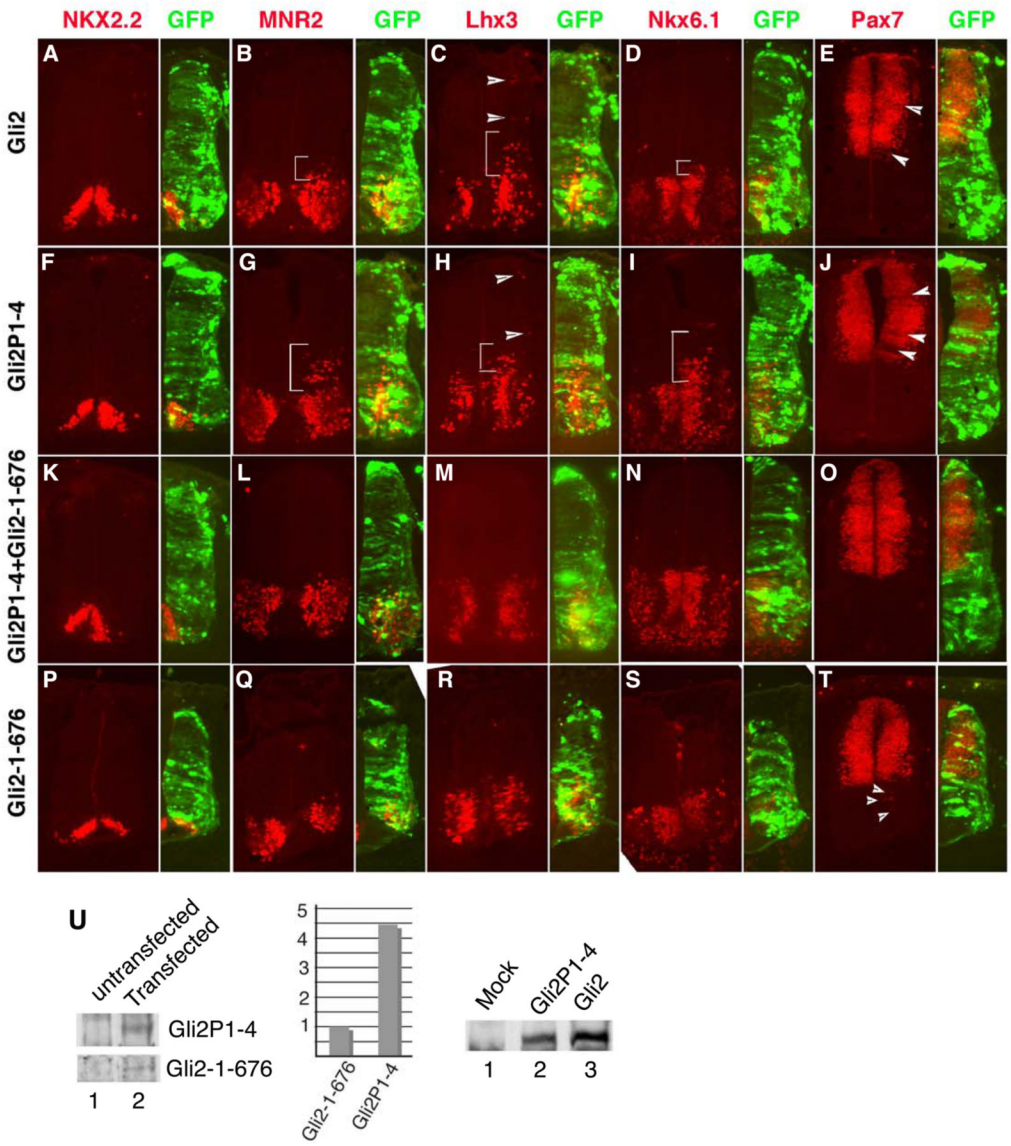

Figure 9. The Gli2 repressor effectively antagonizes the Gli2P1-4 activity

(A–T) Neural tubes of HH stage 12–14 chick embryos were electroporated with GFP and constructs indicated to the left (500 ng for Gli2 and Gli2P1-4, but 20 ng for Gli2-1-676). Following the 48-hr incubation, neural tube sections were prepared and stained with the antibodies shown above the panels. Neural markers that are ectopically activated or suppressed are indicated by brackets or arrowheads. The lateral sides of the neural tubes electroporated are orientated to the right and shown by the double staining of markers and GFP (smaller panels). (U) Immunoblotting analysis of Gli2 protein in embryos un- or co-electroporated with Gli2P1-4 (500 ng) and Gli2-1-676 (20 ng). Upper and lower panels are from the same blot and lanes. Graph in the right shows the quantification of the Gli2 proteins. The right panel shows that levels of Gli2 and Gli3P1-4 expression are comparable.